

⁹⁹Tc NMR of Technetium and Technetium-Ruthenium Metal Nanoparticles

V. P. Tarasov*, Yu. B. Muravlev*, N. N. Popova** and K. E. Guerman**

* *Kurnakov Institute of General and Inorganic Chemistry,
Russian Academy of Sciences, Leninskii pr. 31, Moscow,
119991 Russia*

** *Institute of Physical Chemistry, Russian Academy
of Sciences, Leninskii pr. 31, Moscow, 117915 Russia*

The properties of metals are related to their electronic structure and crystal structure. Small clusters of metal atoms exhibit extraordinary physical and electronic properties, caused by size effects, namely, by the surface-to-volume ratio and discreteness of electronic levels [1]. Bulk technetium metal has a hexagonal close-packed lattice with parameters $a = 2.735$ and $c/a = 1.6047$; technetium films less than 150 \AA thick are characterized by a fcc lattice with $a = 3.68 \text{ \AA}$ [2, 3]. Also, bulk ruthenium metal has a hcp lattice with $a = 2.704 \text{ \AA}$ and $c/a = 1.5809$. Tc–Ru alloys are infinite solid solutions [4]. One of the most important characteristics of the metal electronic structure is the density of states at the Fermi level $N(E_F)$. For the two most probable states of technetium, $(4d^6 5s^1)$ and $(4d^5 5s^2)$, the calculated $N(E_F)$ values are 12.25 and 11.87 states/(Ry atom), respectively [5]. The bulk densities of states in Tc and Ru metal are the same [6]. The experimental characteristics that reflect the metal electronic state and structure are NMR parameters, such as the Knight isotropic shift (K), its anisotropy (K_{an}), spin–lattice relaxation time (T_1), line width ($\Delta\nu$), quadrupole coupling constant (C_Q), and asymmetry parameter η of the electric field gradient tensor. We have recently determined these parameters for a technetium metal powder with a grain size of $50\text{--}100 \text{ \mu m}$: $K = 6872 \text{ ppm}$, $K_{an} = -400 \text{ ppm}$, $(T_1 \times T)^{-1} = 3.23 \text{ s}^{-1} \text{ K}^{-1}$, $C_Q = 5.74 \text{ MHz}$, and $\eta = 0$ [7]. For the bulk ruthenium metal at 4.2 K , the Knight shift is 4900 ppm [8]. We are interested in comparing these characteristics with those for technetium nanoparticles. Here, we present the results of studying technetium and technetium–ruthenium of oxide-supported catalysts by ⁹⁹Tc NMR on supports with different crystal structures and specific surfaces. As is known, small technetium mono- and bimetallic particles on different supports are active catalysts [2]. Metallic active states at the inert oxide support surface are believed to be the cause of catalytic properties of the material formed. In the case of bimetallic catalysts, an increase in catalytic activity (synergism) is due to the formation of intermetallic compounds.

EXPERIMENTAL

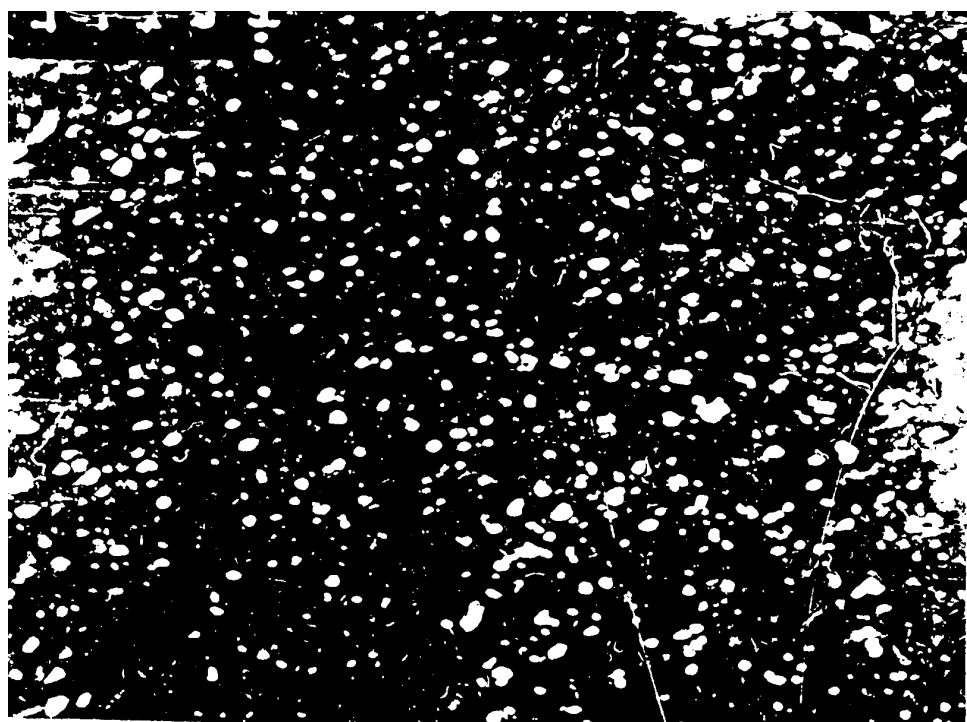
Three types of supports with basic properties were used, namely, γ -Al₂O₃, MgO, and TiO₂ (supports are conventionally classified into acid, basic, and neutral supports [9]). The structure, specific surface S_{sp} , and pore size of these supports are given in Table 1.

Table 1. Characteristic of the supports

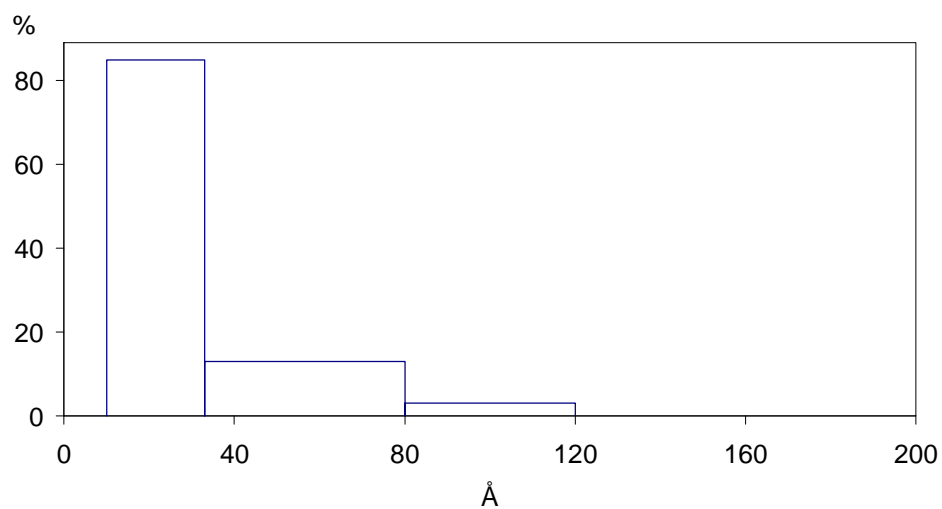
Supports	Structure	Specific surface, S(m ² /g)	Pore size, A
γ -Al ₂ O ₃	spinel	189	320 and 40
MgO	fcc	46	20
TiO ₂	Tetragonal 60% rutile 40% anatase	7	-

The dispersity and particle size of technetium metal were determined on an EM-301 transmitting electron microscope with a resolution of 3.5 Å [10,11]. Fig.1a shows the electron micrograph of a 1% Tc/ γ -Al₂O₃ catalyst, prepared by impregnation; The magnification is 75000. Light spots are technetium nanoparticles. The particles differ in size. Large particles are too infrequent to be visible in the size distribution diagrams, but they may give a non-negligible contribution to the NMR spectrum.

The bar diagrams of size distribution of particles indicate that on a γ -Al₂O₃ support with the highest specific surface, the size of technetium particles ranges from 10 to 80 Å (the average particle size is 23 Å for a 1% Tc/Al₂O₃ catalyst) (Fig.1b). This distribution is skewed toward larger particles with an increase in technetium concentration. For the MgO and TiO₂ supports with a smaller specific surface, size distribution is wider, the average particle size being above 40 Å. Catalysts were prepared by procedures described elsewhere [10, 11]: support samples were impregnated with an



A



B

Fig.1. (a) Electron micrograph of 1 % Tc/ γ -Al₂O₃ catalyst, prepared by impregnation (x75000); (b) Approximate size distribution of Tc particles determined from TEM micrograph in the sample 1 % Tc/ γ -Al₂O₃

aqueous solutions of NH_4TcO_4 and $\text{RuCl}_3 \cdot \text{H}_2\text{O}$ or H_2PtCl_6 , dried at $80\text{--}90^\circ\text{C}$, and reduced in a hydrogen flow for $2\text{--}12$ h at 700°C . The calculated amount of the deposited metal was $\sim 0.01\text{--}20$ wt % for Tc and $1\text{--}10$ wt % for Ru. Catalysts ($0.7\text{--}0.8$ g) were placed in Teflon tubes 10 mm in diameter and 30 mm in length for recording NMR spectra. ^{99}Tc NMR spectra were recorded at 293 K on a Bruker MSL-300 spectrometer in a magnetic field of 7.04 T at a frequency of 67.55 MHz. The spin echo pulse sequence was used. The width of the first exciting pulse was 3.22 μs , repetition time was 0.5 s, and the number of scans was 64000 to 250000 . It is important that the intensity of the signal noticeably depends on the concentration of the initial NH_4TcO_4 solution used for impregnation: for a 0.01 wt % Tc/ Al_2O_3 catalyst, the signal-to-noise ratio was $\sim 2:1$ è was achieved after 2250000 scans with a repetition time of 0.2 s. This spectrum was acquired within a week (Fig.2).

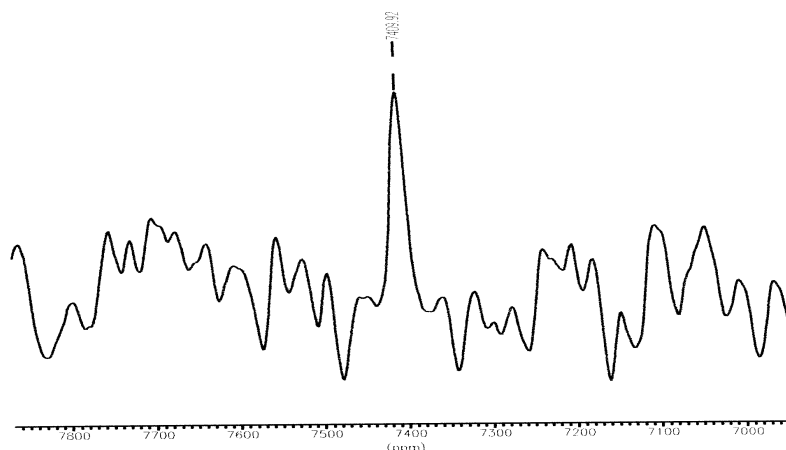


Fig.2. ^{99}Tc NMR spectrum of a 0.01% Tc/ $\gamma\text{-Al}_2\text{O}_3$ catalyst at 295 K, SW 250 kHz, NS 2250000 , $D_0=0.2$ s.

Thus, the plots of Knight shift and line width versus temperature were measured only for a 20% Tc/ Al_2O_3 catalyst. For the same sample, the spin-lattice relaxation time $T_1(^{99}\text{Tc})$ was measured using the standard saturation–recovery technique. The dependence of the peak amplitude of an NMR signal on the delay time is described by a one-exponential function. At 295K , the T_1 is equal to 204 ms, which is about 200 times larger than that for the bulk metal [7]. Chemical shifts were referenced to a 0.1 M KTcO_4 solution as the external standard. Support samples were spherical grains $1.5\text{--}2.0$ mm in diameter.

RESULTS AND DISCUSSION

The ^{99}Tc NMR spectra of all the catalysts under consideration showed signals in the region of technetium metal shifts (~ 7000 ppm) and in the region of the external standard (~ 0 ppm) (ionic form) (Fig. 3a). The integrated intensity of the low-field signal that arose from technetium metal was roughly one order of magnitude weaker than the intensity of the ionic form signal. In the general spectra this signals are hard to observe. The upper spectrum (Fig. 3b) shows this region in more detail.

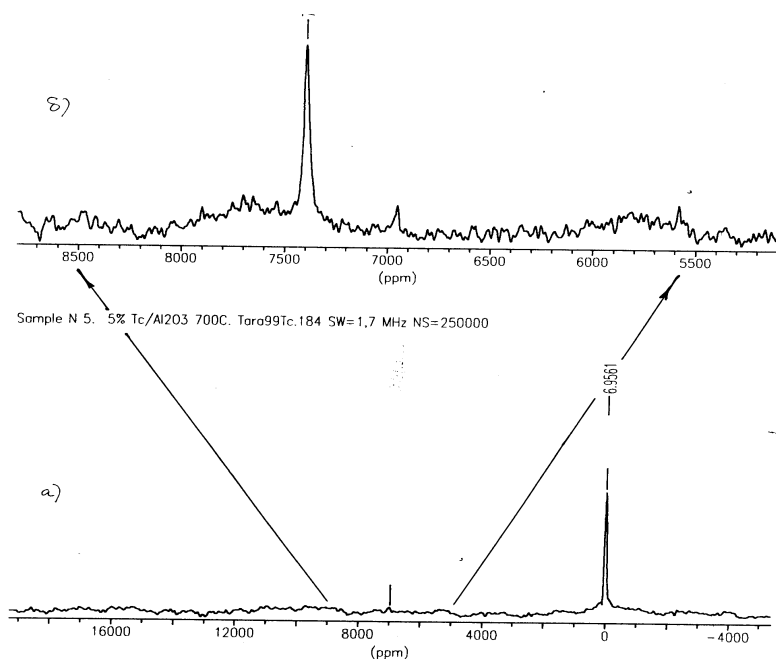


Fig 3. ^{99}Tc NMR spectra of a 5% Tc/ γ - Al_2O_3 catalyst at 295 K;
(a) SW 1.7 MHz, NS 250000, (b) SW 250 kHz, NS 64000,

The stronger signal from small particles has a shift of 7400 ppm. The weaker signal from large particles has a shift of about 6950 ppm. The ^{99}Tc NMR shift and line shape for nanoparticles differ considerably from those for the bulk technetium sample (Fig.4).

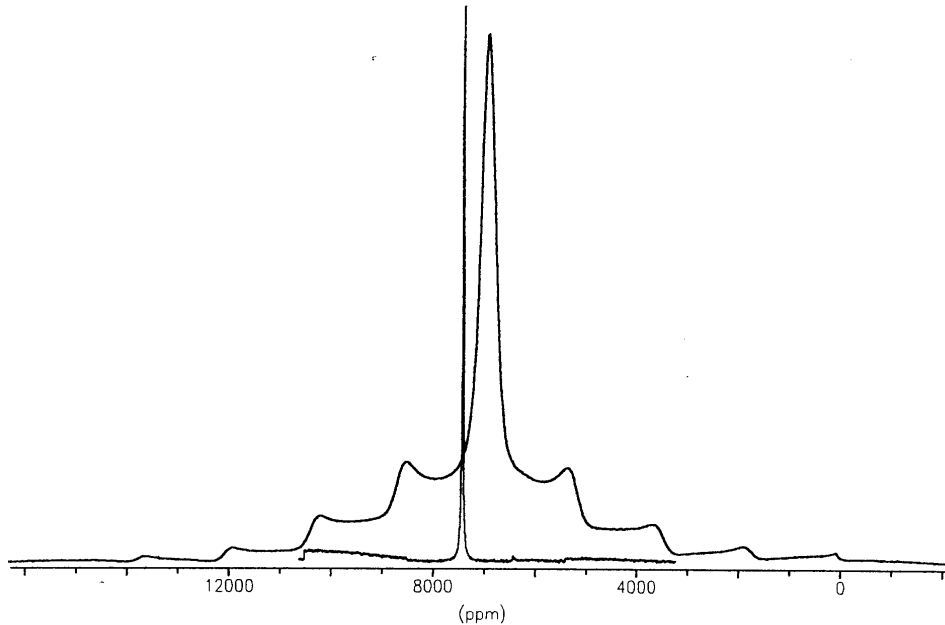


Fig 4. ^{99}Tc NMR spectra of a (a) 20% $\text{Tc}/\gamma\text{-Al}_2\text{O}_3$ catalyst at 295 K; SW 500 kHz, NS 191000, D_0 0.5s ; (b) bulk Tc metal, SW 2.5 MHz, NS 50000, D_0 0.5s.

The shift is 7406 ppm, which is about 600 ppm larger than the shift for the bulk sample. The line with a width at half-maximum of ~ 1 kHz has the Lorentzian shape and lacks the satellite structure caused by first-order quadrupole interactions, typical of the hexagonal close-packed lattice. For technetium foil with $20\mu\text{m}$ thin the ^{99}Tc NMR spectrum shows that the position of the central component is very close to its position in Tc metal powder sample and 8 satellites are not clear due to highly defected crystal cell caused by a mutual consecutive mechanic treatment. The missing quadrupole structure clearly points to the cubic lattice of the nascent technetium phase. The considerable increase in the Knight shift can reflect a change in the density of states at the Fermi level, compared to the bulk technetium sample with the hexagonal close-packed lattice [7]. Figure 5 shows the temperature dependences $K(T)$ of Knight shifts for the bulk sample and technetium nanoparticles.

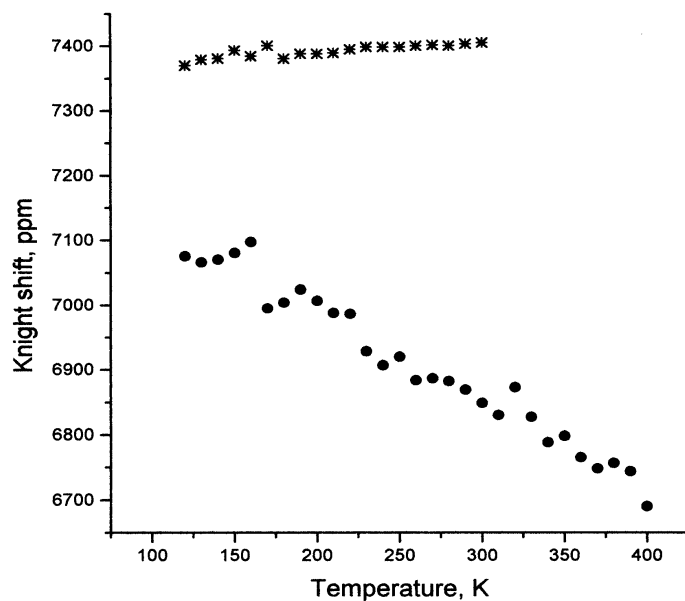


Fig 5. Temperature dependence of the Knight shifts at (a) 20% Tc/ γ - Al₂O₃ catalyst; (b) bulk Tc metal.

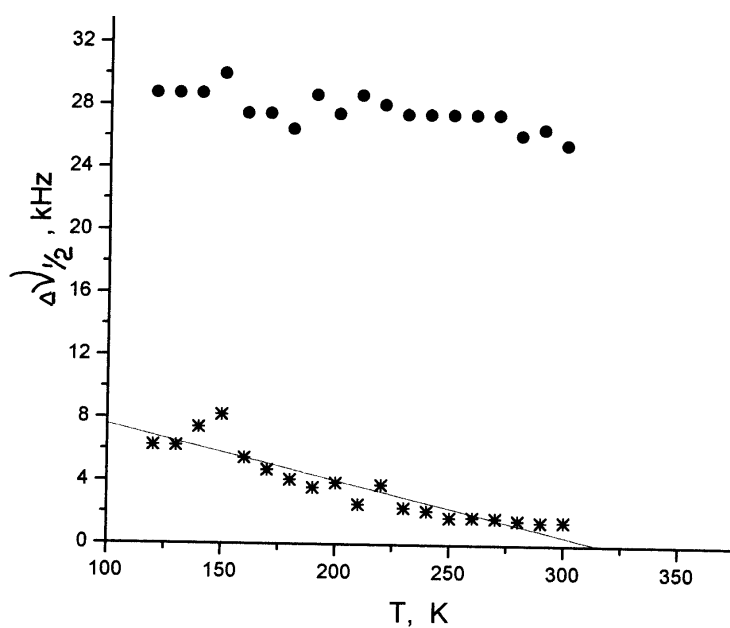


Fig 6. Temperature dependence of the line widths of (a) 20% Tc/ γ - Al₂O₃ catalyst; (b) bulk Tc metal.

Compared to the $K(T) = 7268 - 1.35T$ for the bulk sample, the temperature dependence of the Knight shift for nanoparticles is noticeably weaker, $K(T) = 7360 + 0.16T$, and has the

opposite sign. The plots of linewidth versus temperature for the small particles and bulk technetium are given on fig.6. These dependences are similar and rather weak. For the bulk technetium sample, $K(T)$ is determined by d -polarization interaction on the background of temperature-independent contact and orbital terms [5]. We may assume that for the cubic lattice also, a temperature change in d -polarization contribution dictates a change in the Knight shift. Since the density of d -states for nanoparticles is smaller than for bulk samples [12], the contribution of K_d to the total shift is also smaller in absolute value. However, the reasons behind such a weak temperature dependence $K(T)$ and its reverse sign for nanoparticles, as compared to the bulk technetium sample, are not conclusively established. Table 2-3 presents the ^{99}Tc NMR parameters (Knight shifts for the metal, chemical shifts for the ionic form, line widths, and the metal-to-ionic form content ratio) we measured.

Table2. ^{99}Tc -NMR parameters for $\gamma\text{-Al}_2\text{O}_3$ supported monometallic Tc catalysts

Tc content, %	Annealing time at 700 C, h	NMR shift, ppm		NMR line width, Hz \pm 5%		Integrated intensity ratio Tc/TcO ₄
		Tc metal $K \pm 1.8$	TcO ₄ $\delta \pm 0.2$	Tc metal	TcO ₄	
0.01	12	7409.9	2.8	921.5	937.0	1/14
0.05	12	7411.7	3.6	1215.9	1015.1	1/7
0.1	12	7411.7	3.1	1361.8	898.0	1/4
1	6	7409.9	2.0	1361.8	1053.6	1/17
2	6	7411.7	1.3	1848.2	1443.9	1/12
3	6	7409.9	0.7	1614.7	775.1	1/16
5	12	7409.9	0.2	1653.6	1287.8	1/6
10	2	7408.1	0.5	1848.2	1639.8	1/13
10	6	7409.9	1.6	1365.7	771.2	1/10
20	2	7408.1	0.9	960	878.3	1/8

Table 3a ⁹⁹Tc-NMR parameters for MgO supported monometallic Tc catalysts

Tc content	Annealing time at 700°C, h	NMR shift, ppm		NMR line width, Hz ± 5%		Integrated intensity ratio Tc/TcO ₄
		Tc metal K ±1.8	TcO ₄ δ±0.2	Tc metal	TcO ₄	
1	12	7402.7	-6.0	1611.3	1171.3	1/8
2	12	7406.3	-2.2	2140.0	2420.6	1/13
3	6	7400.9	-8.8	1945.5	1834.1	1/12
4	12	7409.9	-3.8	1848.2	2498.7	1/11
10	12	7406.3	-5.2	3015.5	4060.5	1/8

Table 3b. ⁹⁹Tc-NMR parameters for TiO₂ supported monometallic Tc catalysts

Tc content	Annealing time at 700 C, h	NMR shift, ppm		NMR line width, Hz ± 5%		Integrated intensity ratio Tc/TcO ₄
		Tc metal K ±1.8	TcO ₄ δ±0.2	Tc metal	TcO ₄	
1	2	7431.6	-16.3	4863.7	3434.1	1/17
3	2	7401.2	-13.7	4873.2	3746.3	1/4.7
5	2	7402.7	-1.1	2727.7	1874.0	1/5.5
10	2	7408.1	-1.4	2343.7	1326.8	1/7.7

These data permit the following conclusions: (1) The *K* shifts are independent of the type of a support, within the experimental error; in all the samples technetium metal has a cubic structure. (2) The line widths for the metal and technetium ionic are 1–5 kHz; the lowest values are observed for the γ -Al₂O₃ support, and the highest values, for TiO₂. (3) The shifts for the ionic technetium form are slightly different for the three supports. (4) The metal-to-ionic form ratio slightly depends on the initial technetium concentration, the largest ratio being observed for the TiO₂ support. The high content of the ionic form in the catalyst studied evidently points to the incomplete reduction of the initial salt to the metal, presumably, because of the "capsulation" effect. The stepwise application of the salt to a support would thus be expected to increase the metal content of the catalyst. To verify this hypothesis, we studied three catalysts obtained by layer-by-layer coating of technetium on to a support. The initial sample was 5% Tc/ γ -Al₂O₃ annealed at 700°C for 6 h. This catalyst was then impregnated two times with a 5% salt solution and reduced under identical conditions. The data in Table 4 show that we obtained the result opposite to the expected one; i.e., the content of the ionic form increased. In addition, the signal

due to metal particles became considerably broader and somewhat upfield shifted. This may be due to a wide size distribution of metal particles.

Table 4. ^{99}Tc NMR parameters of three catalysts on $\gamma\text{-Al}_2\text{O}_3$ supports.

Tc content, %	Annealing time at 700°C	NMR shifts, ppm Tc metal	NMR shifts, ppm TcO_2	Line width Tc-metal, Hz	Line width TcO_2 , Hz	Integrated intensity ratio, $I_{\text{Tc}}/I_{\text{TcO}_2}$
5	6	7411.7	3.2	2529	1249	1/3
5 + 5	6	7406,3	3,8	7805	5935	1/14
5 + 5 + 5	6	7406.3	-2.7	4683	3809	1/15

The ^{99}Tc NMR line shape for nanoparticles is represented by an asymmetric contour with a small shoulder at the high-field wing. The degree of asymmetry and the change in line width depend on the technetium concentration and annealing time of the catalyst. However, these changes are irregular (Tables 2–3). The bar diagrams of distribution point to a wide size distribution of particles: from 10 to 80 Å for 1% Tc/ $\gamma\text{-Al}_2\text{O}_3$ (the average diameter is 23 Å) and from 10 to 200 Å for 2% Tc/MgO (the average diameter is 40 Å). The influence of nanoparticle size on the line shape and K has been found for rhodium and platinum [12–14]. Thus, we assumed that the experimental ^{99}Tc NMR line is a composite one because of the size effects of nanoparticles and decomposed this line into components. Simulation of a contour with the LineSim program resulted in five components of the experimental line shape for the 2% Tc/ Al_2O_3 catalyst, in eight components for the bimetallic (3% Tc–1% Ru)/ TiO_2 catalyst and seven components for the 10% Tc–10% Ru/ $\gamma\text{-Al}_2\text{O}_3$ catalyst. Figures 7–9 show the ^{99}Tc NMR spectra and the results of decomposition of experimental lines into components. Each of the components has a Lorentzian shape and a width of 0.5–1.0 kHz. The area under a component corresponds to the relative concentration of a definite technetium metal form. Table 5 shows the results for two Tc–Ru catalysts and a 3% Tc–3% Pt/MgO catalyst.

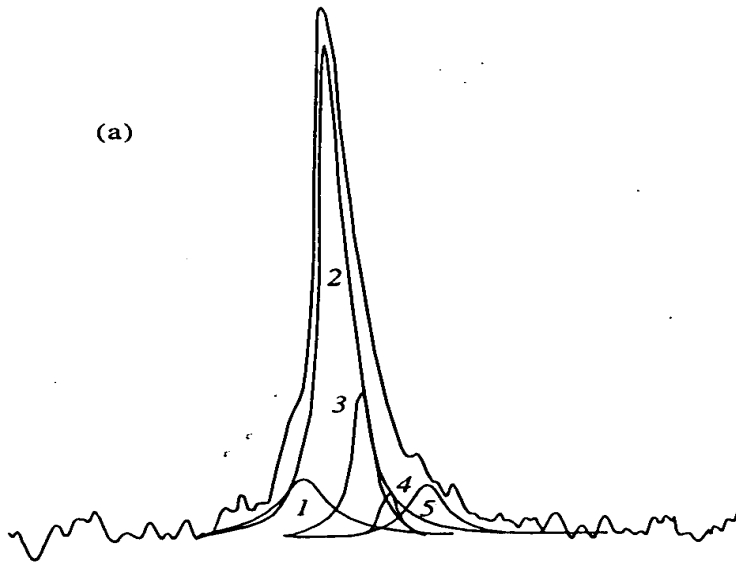
Table 5. ^{99}Tc -NMR parameters for $\gamma\text{-Al}_2\text{O}_3$ and TiO_2 supported bimetallic Tc catalysts

Tc content	Annealing time at 700°C, h	NMR shift, ppm		NMR line width, Hz \pm 5%		Integrated intensity ratio Tc/TcO ₄
		Tc metal K \pm 1.8	TcO ₄ $\delta \pm 0.2$	Tc metal	TcO ₄	
for 10% Ru–10% Tc on $\gamma\text{-Al}_2\text{O}_3$						
10	6	7410.2	0.9	2075.2	1281.7	1/4.5
for 1% Ru–3% Tc on TiO_2						
3	2	7395.5	-15.2	4263.8	3118.5	1/4.6
for 3% Pt–3% Tc on MgO						
3	12	7399.4	-11.7	3440.0	4018.5	1/13

As can be seen, neither the type of support nor the nature of the second metal has a little effect on the ^{99}Tc NMR line width and shift. This may be an indication of the absence of any intermetallic compounds in the catalysts studied.

Consideration of the size distributions of particles in combination with the intensities and shifts of resonance lines permits the tentative and qualitative conclusion that the smaller the technetium nanoparticles, the larger the Knight shift (downfield shift). In a small particle, the technetium positions are not equivalent, in contrast to the bulk sample where translational symmetry results in equivalent technetium positions. Site nonequivalence implies that the densities of states N_s and N_d change in switching from one technetium position to another. In this case, N_s and N_d are related to the local density of states [13]. Therefore, each technetium position gives rise to an individual relatively narrow (< 1 kHz) line, and the experimental spectrum is an unresolved superposition of these individual lines. The model for describing the Knight shift is based on the concept of layer nonequivalence of atoms [14]. Each technetium layer is treated as a spherical shell 2.5-3 Å thick. For the cubic lattice, the smallest particle contains 13 atoms: one atom is at the center, and 12 atoms are at the surface. The next layer contains 42 atoms, etc. The overall number of atoms in a particle containing $(m + 1)$ layers is $N_T(m + 1) = N_T(m) + N_S(m + 1)$, where $N_T(m) = 10/3 m^3 - 5m^2 + 11/3m - 1$ is the number of atoms in the interior layers, and $N_S = 10m^2 + 2$ is the number of atoms at the surface of a layer [11]. For spherical

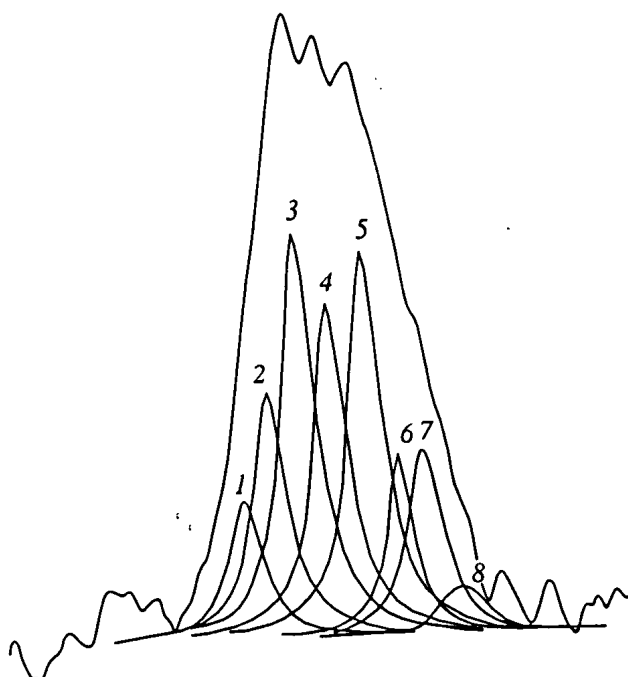
technetium nanoparticles with an average diameter of 20 to 40 Å, the number of atoms is 100 to 2000, which corresponds to the number of layers from 4 to 8. For each layer, the Knight shift K_n is the same. The layer with $n = 0$ corresponds to the surface, the layer with $n = 1$ corresponds to the subsurface layer, etc. The Knight shift for the n th layer K_n is described by the formula [15]: $K_n - K_\infty = (K_0 - K_\infty) \exp(-n/m)$, where $K_\infty = 7350$ ppm is the limiting shift of the technetium position in the bulk, $K_0 = 7430$ ppm is the technetium shift at the surface of a particle with a given diameter, m is a dimensionless constant, which has the meaning of the depth at which the layers have distinguishable Knight shifts. With allowance for these data, the Knight shifts K_n in the layers of a five-layer particle were estimated to be $K_1 = 7417$, $K_2 = 7410$, $K_3 = 7397$, $K_4 = 7384$, and $K_5 = 7365$ ppm, at the average value $m = 5$. The calculated K_n values are consistent with the data obtained upon decomposition of the experimental line shape (table to Fig. 7).



Peak No	Knight shift, ppm	Line width, Hz	Peak intensity	Signal area, %
1	7431.2	1955.0	11.5	11.4
2	7411.4	1309.5	93.3	65.4
3	7399.5	892.1	27.5	13.1
4	7385.0	420.3	9.2	2.1
5	7365.6	1538.9	9.8	9.1

Fig. 7. ^{99}Tc NMR spectrum of a 2%Tc/ $\gamma\text{-Al}_2\text{O}_3$ catalyst and its decomposition into Lorentzian components; the NMR parameters of the components and their intensities are given in the table.

Note that the layer model for a monodisperse sample implies that the most intense signal with the maximal shift K_o should arise from the surface. The signals that arise from interior layers will be less intense. The real sample is polydisperse, which may lead to a change in K_o depending on the particle size, so that the intensity distribution is disturbed. For the binary (3% Tc–1% Ru)/TiO₂ and 10% Tc-10% Ru/ γ -Al₂O₃, the experimental line shape points to the multicomponent character of the signal (Fig. 8 and 9).



Peak No	Knight shift, ppm	Line width, Hz	Peak intensity	Signal area, %
1	7427.3	885.1	22.3	7.1
2	7418.1	925.0	39.8	18.2
3	7408.2	872.1	65.5	20.6
4	7396.2	909.2	54.5	17.9
5	7384.8	909.8	62.2	20.4
6	7378.3	791.5	29.2	8.3
7	7364.1	916.8	29.9	9.9
8	7351.1	919.8	7.7	2.6

Fig. 8. ⁹⁹Tc NMR spectrum of a binary 1% Ru - 3%Tc/TiO₂ catalyst and its decomposition into Lorentzian components; the NMR parameters of the components and their intensities are given in the table.

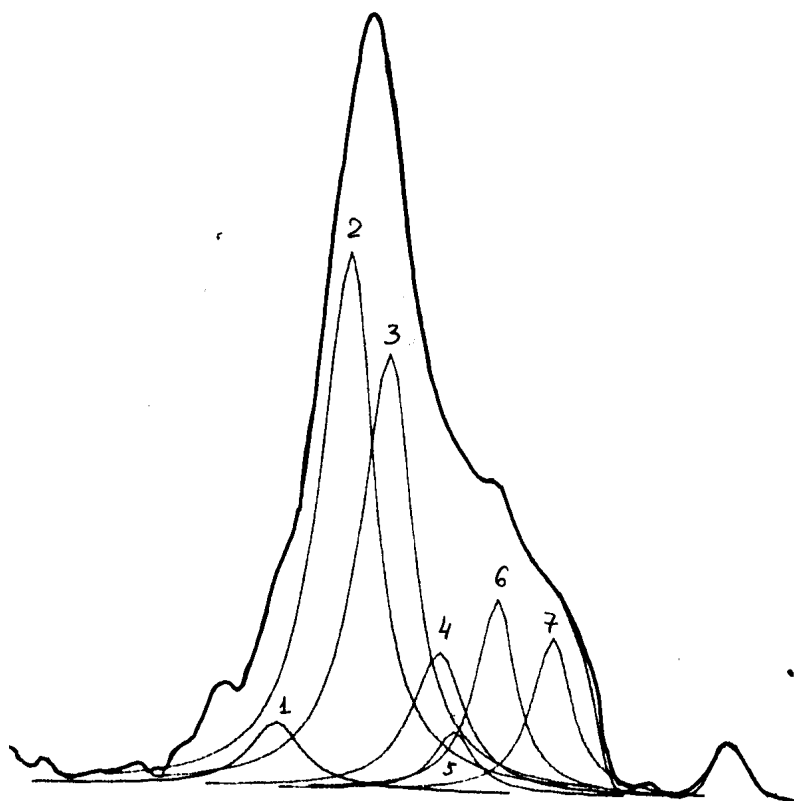


Fig. 9. ^{99}Tc NMR spectrum of a binary 10% Ru - 10%Tc/ $\gamma\text{-Al}_2\text{O}_3$ catalyst and its decomposition into Lorentzian components; the NMR parameters of the components and their intensities are given in the table.

Peak Number	Knight shift, ppm	Line width, Hz	Peak intensity	Signal area, %
1	7429.3	994.0	8.5	4.3
2	7414.5	1007.0	68.9	35.4
3	7406.3	1037.9	56.0	29.7
4	7393.4	1071.5	17.9	9.8
5	7389.9	665.8	7.8	2.6
6	7381.0	814.9	24.9	10.3
7	7367.6	762.9	20.1	7.8

A possible reason for this observation may be the narrower individual lines due to dilution of technetium with ruthenium. Since the width of each individual line is determined by dipole-

dipole interaction between the magnetic moments of technetium spins, substituting ruthenium, characterized by low natural abundances of magnetic isotopes with small magnetic moments, for a fraction of technetium will lead to line narrowing.

As was mentioned above, the spectra show the signals of the ionic form, along with the signals due to the metal. The ^{99}Tc NMR chemical shift of this form corresponds to the shift of the pertechnetate ions, and the counterion may be ammonium or the positive charge of the support. To decide between these possibilities, we studied the ^1H and ^{14}N NMR spectra of a 5% Tc/ Al_2O_3 catalyst, depending on the annealing time in a hydrogen atmosphere. We found that the integrated intensities of ^1H and ^{14}N NMR signals decreased with an increase in annealing time from 2 to 12 h at 700°C. A ^1H NMR signal was observed for all the catalysts and initial supports. The signal was a two-component line with a width of ~4 kHz. The signal became weaker after annealing a sample. The ^{14}N NMR chemical shift was 300 ppm from the signal of ammonium in an aqueous NH_4NO_3 solution. Therefore, we assigned the signal of the ionic form to residual unreduced ammonium pertechnetate. The smallest amount of unreduced NH_4TcO_4 was found for the TiO_2 support, which may be due to specific features of its surface (the pore number and size). For TiO_2 , the specific surface is two orders of magnitude lower than for the remaining supports (Table 1). Therefore, the latter may exhibit the “encapsulation” effect when a fraction of the initial component (NH_4TcO_4) is caught in pores and, thus, is not reduced. As follows from Tables 2–4, the content of unreduced technetium (ionic form) exceeds the content of the metal phase roughly tenfold.

It should be noted that the question of the nature of the ionic form in the catalysts under consideration is still open [16], since the ^{99}Tc NMR shifts are the same for TcO_2 and NH_4TcO_4 powders.

REFERENCES

1. Halperin, W.P., *Rev. Mod. Phys.*, 1986, vol. 58, no. 3, p. 533.
2. Spitsin, V.I., Kuzina, A.F., Pirogova, G.N., and Balakhovskii, O.A., *Itogi Nauki Tekh., Ser.: Neorg. Khim.*, 1984, vol. 10.
3. Golyanov, V.M., Elesin, L.A., and Mikheeva, N.M., *Zh. Eksp. Teor. Fiz.*, 1973, vol. 18, p. 572.
4. Zaitseva, L.L., Velichko, A.V., and Vinogradov, I.V., *Itogi Nauki Tekh., Ser.: Neorg. Khim.*, 1984, vol. 9.
5. Faulkner, J.S., *Phys. Rev.*, 1977, vol. 16, no. 2, p. 736.

6. Van der Klink J.J. *Adv. Catal.*, 2000, vol. 44, p. 1
7. Tarasov, V.P., Muravlev, Yu.B., and Guerman, K.E., *J. Phys.: Condens. Matter* 2001, vol. 13 (in press).
8. Burgstaller A., Ebert H., Voitlander J. // *Hyperfine Interactions*, 1986, vol. 89, p. 1015
9. Stakheev, A.Yu. and Kustov, L.M., *Appl. Catal. A*, 1999, vol. 188, p. 3.
10. Pirogova, G.N., Popova, N.N., Matveev, V.V., and Chalykh, A.E., *Izv. Akad. Nauk SSSR, Ser. Khim.*, 1990, no. 11, p. 2486.
11. Pirogova, G.N., Popova, N.N., Voronin, Yu.V., *et al.*, *Zh. Fiz. Khim.*, 1990, vol. 64, no. 11, p. 2933.
12. Tong, Y.Y., Yonezawa, T., Toshima, N., and Van der Klink, J.J., *J. Phys. Chem.*, 1996, vol. 100, no. 2, p. 730.
13. Vuissoz, P.A., Yonezawa, T., Yang, D., *et al.*, *Chem. Phys. Lett.*, 1997, vol. 264, p. 366.
14. Bucher, J.P., Buttet, J.J., and Van der Klink, J.J., *Surf. Sci.*, 1989, vol. 214, p. 347.
15. Makowka, C.D., Slichter, C.P., and Sinfelt, J.H., *Phys. Rev. B: Condens. Matter*, 1985, vol. 31, p. 5663.
16. Chinenov P.P., Ronyi S.I., Ershov V.V. *et al.* *Radiokhimiya*, 1997, vol. 39, no. 3, p. 219.